**Astronomy
&
Astrophysics**

On the relation of optical obscuration and X-ray absorption in Seyfert galaxies

L. Burtscher[1], R. I. Davies[1], J. Graciá-Carpio[1], M. J. Koss[2], M.-Y. Lin[1], D. Lutz[1], P. Nandra[1], H. Netzer[3],
G. Orban de Xivry[1], C. Ricci[4], D. J. Rosario[1], S. Veilleux[5,6], A. Contursi[1], R. Genzel[1], A. Schnorr-Müller[1],
A. Sternberg[7], E. Sturm[1], and L. J. Tacconi[1]

[1] Max-Planck-Institut für extraterrestrische Physik, Postfach 1312, Gießenbachstr., 85741 Garching, Germany
    e-mail: burtscher@mpe.mpg.de
[2] Institute for Astronomy, Department of Physics, ETH Zürich, Wolfgang-Pauli-Strasse 27, 8093 Zürich, Switzerland
[3] School of Physics and Astronomy, Tel Aviv University, 69978 Tel Aviv, Israel
[4] Instituto de Astrofísica, Facultad de Física, Pontificia Universidad Católica de Chile, 306, Santiago 22, Chile
[5] Department of Astronomy, University of Maryland, College Park, MD 20742, USA
[6] Joint Space-Science Institute, University of Maryland, College Park, MD 20742, USA
[7] Raymond and Beverly Sackler School of Physics & Astronomy, Tel Aviv University, 69978 Ramat Aviv, Israel

ABSTRACT

The optical classification of a Seyfert galaxy and whether it is considered X-ray absorbed are often used interchangeably. There are many borderline cases, however, and also numerous examples where the optical and X-ray classifications appear to be in disagreement. In this article we revisit the relation between optical obscuration and X-ray absorption in active galactic nuclei (AGNs). We make use of our "dust colour" method to derive the optical obscuration A_V, and consistently estimated X-ray absorbing columns using 0.3–150 keV spectral energy distributions. We also take into account the variable nature of the neutral gas column N_H and derive the Seyfert subclasses of all our objects in a consistent way. We show in a sample of 25 local, hard-X-ray detected Seyfert galaxies ($\log L_X/(\mathrm{erg/s}) \approx 41.5-43.5$) that there can actually be a good agreement between optical and X-ray classification. If Seyfert types 1.8 and 1.9 are considered unobscured, the threshold between X-ray unabsorbed and absorbed should be chosen at a column $N_H = 10^{22.3}$ cm^{-2} to be consistent with the optical classification. We find that N_H is related to A_V and that the N_H/A_V ratio is approximately Galactic or higher in all sources, as indicated previously. However, in several objects we also see that deviations from the Galactic ratio are only due to a variable X-ray column, showing that (1) deviations from the Galactic N_H/A_V can be simply explained by dust-free neutral gas within the broad-line region in some sources; that (2) the dust properties in AGNs can be similar to Galactic dust and that (3) the dust colour method is a robust way to estimate the optical extinction towards the sublimation radius in all but the most obscured AGNs.

Key words. galaxies: active – galaxies: nuclei – galaxies: Seyfert – dust, extinction

1. Introduction

Seyfert galaxies are commonly classified by the presence or absence of broad permitted emission lines in the optical, though finer classification schemes exist to differentiate between the various types of broad-line galaxies. A complementary classification scheme is provided by space-based X-ray observations which allow us to determine the equivalent neutral hydrogen absorbing column N_H towards the compact X-ray emitting corona around the central black hole. The result of these phenomenological classifications is a great apparent diversity of active galactic nuclei (AGNs).

The most successful approach to understanding this menagerie of AGN types is unification by orientation (Rees 1966). Polarized, i.e. scattered, broad lines are probably the strongest indication for a torus, i.e. toroidal obscuration by dust (Antonucci & Miller 1985) blocking our line of sight towards the broad-line region (BLR) at some inclinations. Strong support for a confining structure on small scales also comes from observations of well-defined ionization cones (e.g. Schmitt et al. 2003).

For a comprehensive overview of the concept of the torus we refer to the recent review by Netzer (2015).

Many observational tests have challenged the unified model. For example, claims for obscured (type 2) AGNs without hidden BLRs have been made (Tran 2001), but recent investigations have shown that most of these objects actually do show broad lines in polarized light if sensitivity is carefully taken into account (Ramos Almeida et al. 2015). Objects that intrinsically lack a BLR (dubbed "true type 2") are rare (Panessa & Bassani 2002) and most of them turn out to be either ordinary type 2s (with a substantial column of neutral gas) or faint type 1s if examined carefully (Shi et al. 2010).

However, there are clearly exceptions to the rule, such as type 1 AGNs in edge-on configurations (e.g. NGC 3783, Müller-Sánchez et al. 2011). This argues in favour of statistical unification where an AGN is more likely to be observed as a broad-line (type 1) AGN if its torus has a larger opening angle or a smaller number of clouds as shown by fitting of the Spectral Energy Distribution (SED) with clumpy torus models (Ramos Almeida et al. 2011; Elitzur 2012).

It is also a matter of debate exactly where the obscuring structure is located. While infrared continuum reverberation mapping and interferometry have shown that the hot and warm dust are located on (sub-)parsec scales (e.g. Burtscher et al. 2013, and references therein), geometrically thick gas structures are also found on the slightly larger (∼30 pc) scales of nuclear star clusters (Hicks et al. 2009) and there is also evidence in a few Compton-thick galaxies that a substantial amount of obscuration might be contributed by the host galaxy since some of the deepest silicate absorption features are seen in edge-on galaxies (Goulding et al. 2012).

Much of the uncertainty arises from different tracers of the obscuration/absorption down to the nucleus and may lead to inconsistent classification across the electromagnetic spectrum (e.g. Merloni et al. 2014). While some of this inconsistency may be caused by dust-free, neutral absorption in the torus (Davies et al. 2015), it should be kept in mind that the different tracers are susceptible to various problems, e.g. the effects of host galaxy dilution and contamination, or the details of X-ray spectral modelling.

In this work, we use a new measure of the near-IR-mid-IR (NIR-MIR) extinction (Burtscher et al. 2015), which is more sensitive to high dust columns than purely optical methods. We also use the best available X-ray spectral modelling results for a well-defined sample of local AGNs. We include a consistent classification of Seyfert types and – more importantly – take into account the temporal variability of the X-ray absorbing column. With this, we explore the relationships between the X-ray and optical obscuration in a more rigorous way than ever done before. We compare the columns of gas and dust that the different tracers of obscuration imply and discuss what this means for the concept of the torus and its structure.

The paper is organized as follows: we briefly introduce the sample and method (Sect. 2) and then study the relation between the optically classified Seyfert type and X-ray absorption (Sect. 3); we study the relation between optical obscuration and the X-ray absorbing column and discuss its implications (Sect. 4).

2. Sample and analysis

Our selection is based on the sample presented in Burtscher et al. (2015, hereafter B15). There we used essentially all local ($D \lesssim 60$ Mpc) AGNs observed with VLT/SINFONI integral field spectroscopy in the near-IR K band. Here we additionally require the source to be detected in the BAT 70-month survey (Baumgartner et al. 2013) in order to have consistent N_H estimates using 0.3–150 keV spectral energy distributions (Ricci et al. 2015.)[1]. We include three additional BAT-detected AGNs (ESO 137-G034, NGC 5728 and NGC 7213) which have new

VLT/SINFONI data from our ongoing observing programme (Davies et al. 2015). The sample and some relevant properties are listed in Table 1.

For these sources we derive the fraction of near-infrared non-stellar light f_{AGN}^{NIR} using the level of dilution of the stellar CO(2, 0) absorption profile at 2.29 μm as a proxy for the AGN light. Here, we summarize briefly the method used to derive the extinction and refer the reader to B15 for more details.

The temperature is estimated from a fit to the K-band spectrum using a stellar template and a black body. To derive the optical extinction to the hot dust we use a simple torus model involving a hot ($T \approx 1300$ K) and a warm ($T = 300$ K) component. By assuming that the intrinsic temperature of the hot dust is roughly a constant, set by the sublimation of dust rather than by the chances of matter distribution, we can explain cooler temperatures and redder near-to-mid-infrared colours ($K - N$) by an absorber with extinction A_V. The derived extinction as a function of the observed colour temperature in the near-IR is shown in Fig. 1. Since the absorber is likely the parsec-scale torus and therefore ≈4–20 times larger than the sublimation radius (Burtscher et al. 2013), screen extinction appears to be a suitable absorbing geometry. This is also valid for a clumpy torus where the near-IR emission is still expected to be significantly more compact than the mid-IR emission (e.g. Fig. 6 in Schartmann et al. 2008).

For this article we use the average observed colour temperature of optical broad-line AGNs (types 1.0–1.9) in this sample as the intrinsic temperature of the hot dust. It is $T_1 = 1311 \pm 129$ K. This scatter in observed intrinsic colour temperatures translates to an uncertainty in A_V of about 3 mag (see Fig. 1) and constitutes the dominant factor in the uncertainty of A_V.

Four of the sources in this selection do not show an AGN continuum in the SINFONI data, despite being detected by *Swift*/BAT in the very hard X-ray band 14–195 keV; therefore, we cannot derive an optical extinction for ESO 137-G034[2], NGC 5643, NGC 5728, and NGC 7130 using our method. All of these sources have Compton-thick ($\log N_H/\mathrm{cm}^2 > 24.2$) neutral absorbers, suggesting that the hot dust may be obscured even at infrared wavelengths.

Compared to other methods of estimating the extinction towards the central engine of AGNs, our method has the advantage of being much simpler. We only require a measurement of the K-band continuum at high spatial resolution such as can be provided with about 10 min of VLT/SINFONI time, for example. In order to apply the more widely used method using broad hydrogen recombination lines, on the other hand, multiple lines must be observed simultaneously in order to constrain both the dust reddening and the ionization properties in the BLR since "case B" (Osterbrock & Ferland 2006) is not applicable there (e.g. La Mura et al. 2007; Dong et al. 2008). Such data rarely exist and so spectra are either stitched together from multiple epochs of observations (with all the caveats regarding variability) or case B has to be assumed for the intrinsic line ratios which effectively leads to an upper limit of the actual obscuration (e.g. Maiolino et al. 2001).

3. Seyfert subtype and X-ray absorption

In order to investigate the relation between Seyfert sub-type and X-ray classification, we need to choose a classification scheme.

---

[1] The baseline model that was used for the spectral fitting (in the 0.3–150 keV band) included an absorbed cutoff power-law continuum plus a reflection component (PEXRAV in XSPEC). For unobscured sources ($\log N_H/\mathrm{cm}^2 \lesssim 22$) we added, if statistically needed, a black body component (for the soft excess), a cross-calibration constant (for possible variability between the non-simultaneous soft X-ray and BAT observations), and an iron line (or other emission lines in the Fe region). Partially covering ionized absorption was taken into account in the spectral analysis using the ZXIPCF model in XSPEC. For obscured sources we added a scattered component, a collisional plasma, emission lines, and a cross-calibration constant. The N_H values quoted here refer to the cold absorber only, since we believe that the warm absorber is related instead to the outflowing component and probably located on scales larger than the BLR/torus absorption.

[2] The CO map in ESO 137-G034 is complex and so no estimate for the AGN fraction can be given using this method. A spectral fit, however, does not show any indication for a hot near-IR continuum.

Table 1. Sample properties.

ID	$f_{\rm AGN}^{\rm NIR}$	T	$A_{\rm V}$	$\log N_{\rm H}$ BAT	$\log N_{\rm H}$ variable	Seyfert type	[OIII]λ5007/Hβ
		[K]	[mag]		[cm^{-2}]		
Circinus galaxy	0.77	691	27.2	24.4	–	1h[a]	–
ESO 137-G034	<0.1	–	–	24.3	–	2[b]	–
ESO 548-G081	0.87	1236	1.6	<20.0	–	1.0	5.5[c]
IC 5063	0.56	947	11.3	23.6	23.3[1]–23.4[1]	1h[d]	–
MCG -05-23-16	0.86	1207	2.3	22.2	22.1[1]–22.7[1]	1.9	0.07[e]
NGC 1052	0.24	1239	1.5	23.0	–	1h[f]	–
NGC 1068	0.92	723	24.6	25.0	–	1h[g]	–
NGC 1365	0.94	1282	0.4	22.2	22.0[2]–25.0[1]	1.8	0.08[e]
NGC 1566	0.57	1479	0.0	<20.1	<20.1[4]–21.9[12]	1.5	0.91[h]
NGC 2110	0.81	967	10.5	23.0	22.5[3]–22.9[4]	1h[s]	–
NGC 2992	0.61	1111	5.1	21.7	21.6[1]–22.2[1]	1.8	0.09[e]
NGC 3081	0.37	977	10.0	23.9	23.7[1]–23.8[1]	1h[i]	–
NGC 3227	0.67	1543	0.0	21.0	21.0[4]–23.4[5]	1.5	0.37[j]
NGC 3281	0.83	732	23.9	23.9	–	2[k]	–
NGC 3783	0.99	1244	1.3	20.5	20.5[4]–23.0[6]	1.5	1.07[e]
NGC 4051	0.64	1305	0.0	<19.6	–	1.5	1.1[l]
NGC 4388	0.78	887	14.2	23.5	23.3[7]–23.8[7]	1h[m]	–
NGC 4593	0.88	1292	0.2	<19.2	–	1.5	1.85[e]
NGC 5128	0.82	796	19.4	23.1	22.8[8]–23.2[8]	2[n]	–
NGC 5506	0.99	1223	1.9	22.4	22.3[1]–22.7[1]	1i[o]	–
NGC 5643	<0.1	–	–	25.4	–	2[k]	–
NGC 5728	<0.1	–	–	24.2	–	2[k]	–
NGC 6300	0.53	677	28.4	23.3	23.3[1,9]–25.0[10]	2[k]	–
NGC 6814	0.58	1500*	0.0	21.0	–	1.5	0.55[h]
NGC 7130	<0.1	–	–	24.0	–	1.9[p]	–
NGC 7172	0.7	822	17.8	22.9	22.9[1]–23.0[1]	1i[q]	–
NGC 7213	0.81	1181	3.0	<20.4	–	1.5	0.79[h]
NGC 7469	0.88	1355	0.0	20.5	–	1.0	6.5[r]
NGC 7582	0.89	1082	6.1	24.2	22.7[1]–24.1[11]	1i[s]	–

Notes. $f_{\rm AGN}^{\rm NIR}$: fraction of non-stellar flux in the K band within an aperture of 1″ (for most sources); T: temperature of a black body from a fit to the K-band spectrum (for errors on $f_{\rm AGN}^{\rm NIR}$ and T, see B15); $A_{\rm V}$: extinction towards the hot dust (from B15; error is estimated to be 3 mag, see Sect. 2); $N_{\rm H}$: X-ray absorbing column from Ricci et al. (2015). (formal errors are <0.2 dex); $N_{\rm H}$ variable: full range of other published $N_{\rm H}$ values for these sources; *Seyfert type*: for broad-line galaxies (1.0/1.2/1.5) based on the Hβ/[OIII]λ5007 ratio (see reference there) and converted to a Seyfert type according to the Winkler (1992) scheme, Seyfert 1.8/1.9: Osterbrock (1981), 1i: broad hydrogen recombination line(s) detected at infrared wavelengths, 1h: broad hydrogen recombination line(s) detected in polarized optical light; 2: no broad hydrogen recombination line detected. * New observations with adaptive optics for NGC 6814 show much hotter dust in this source than in B15. The origin of this discrepancy is unknown and might be related to intrinsic variability. Here we adopt an intermediate value, effectively reducing the adopted $A_{\rm V}$ from 7.2 to 0.

References. *X-ray variability:* [1]: Risaliti et al. (2002), [2]: Walton et al. (2014), [3]: Rivers et al. (2014), [4]: Ricci et al. (in prep.), [5]: Lamer et al. (2003), [6]: Markowitz et al. (2014), [7]: Fedorova et al. (2011), [8]: Beckmann et al. (2011), [9]: Guainazzi (2002), [10]: Leighly et al. (1999), [11]: Bianchi et al. (2009), [12]: Kawamuro et al. (2013). *Seyfert types and line ratios:* [a] Oliva et al. (1998); [b] Véron-Cetty & Véron (2010); [c] Koss et al., in prep.; [d] Lumsden et al. (2004); [e] Schnorr-Müller et al., in prep.; [f] Barth et al. (1999); [g] Antonucci & Miller (1985); [h] Winkler (1992); [i] Moran et al. (2000); [j] Smith et al. (2004); [k] Phillips et al. (1983); [l] Grupe et al. (2004); [m] Shields & Filippenko (1996); [n] Tadhunter et al. (1993); [o] Nagar et al. (2002); [p] Storchi-Bergmann et al. (1990); [q] Smajić et al. (2012); [r] Kim et al. (1995); [s] Reunanen et al. (2003).

Perhaps the most physical scheme is the one by Osterbrock (1977), which subdivides the population into Seyfert 1.0, 1.2, and 1.5 according to the prominence of the broad compared to the narrow component of Hβ. Since isolation of the broad component of Hβ is sometimes difficult, however, alternative schemes use the total Hβ flux and compare it to the flux in the [OIII]λ5007 line (Whittle 1992; Winkler 1992). This flux ratio also probes the dominance of direct AGN emission (broad Hβ) over isotropic AGN emission ([OIII]λ5007) from the narrow line region, but both lines can be contaminated by star formation. It is expected that these contaminations cancel out to some

degree, which may explain the popularity of this indicator for classifying Seyfert galaxies. For this work, we use the Winkler (1992) scheme[3].

Additionally, the classifications 1.8 and 1.9 are given if [OIII]λ5007/Hβ > 3, but weak broad lines – Hα and Hβ or only Hα, respectively – are seen (Osterbrock 1981). We use the classification "type 1i" for AGNs that show broad hydrogen recombination lines at infrared wavelengths and finally there are also

---

[3] This scheme is also employed by Véron-Cetty & Véron (2010) on which much of the SIMBAD and NED classifications are based.
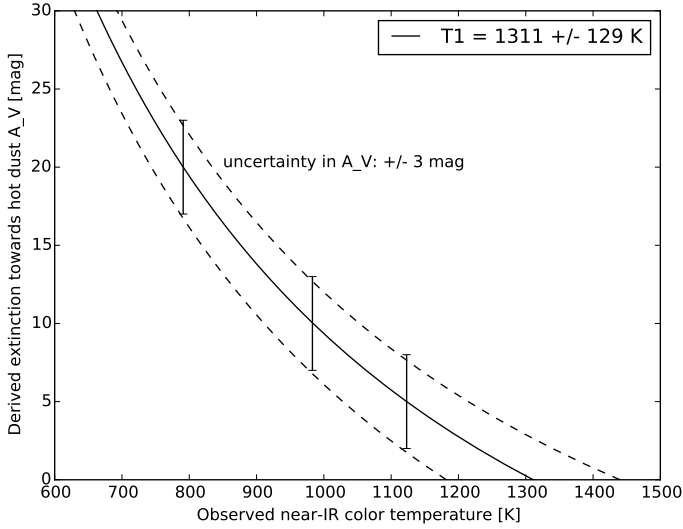
Fig. 1. Derived extinction towards the hot dust A_V vs. observed near-IR colour temperature. The intrinsic temperature T_1 is set by the observed colour temperature of presumably unobscured sources (Seyfert 1.0–1.5) and the spread in these observed temperatures translates into an uncertainty of A_V of about 3 mag as indicated for several observed colour temperatures. For details of the fit of the near-IR colour temperature we refer to B15, specifically Fig. 6 there.
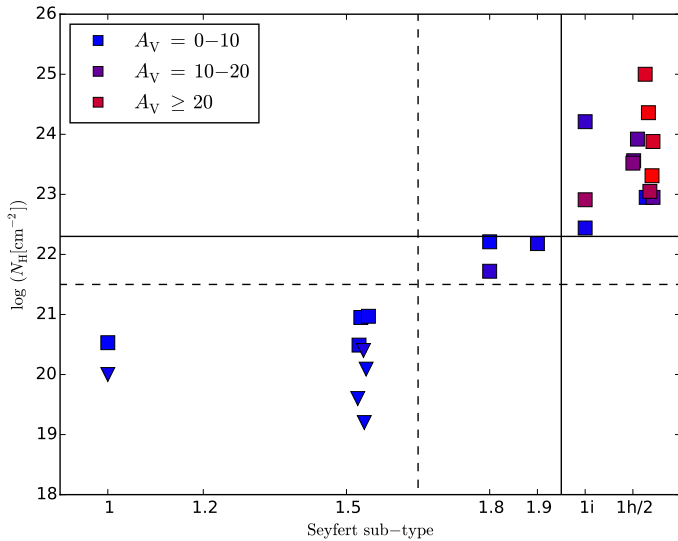
Fig. 2. X-ray absorbing column N_H vs. Seyfert subtype. The symbols for subtypes 1.5 and 2 have been randomly shifted by a small amount for better readability. The symbol colour indicates the optical obscuration to the hot dust. The solid and dashed lines indicate two possible consistent dividing lines between optically unobscured/obscured and X-ray unabsorbed/absorbed.

Seyfert galaxies of "type 1h" where these lines are only seen in polarized optical light. The resulting classifications are given in Table 1.

In Fig. 2 we compare these classifications with the X-ray absorbing column N_H (Ricci et al. (2015).) and find a correlation in the expected sense. It is evident that there is a clear separation between broad-line and narrow-line AGNs in the X-ray absorbing column with intermediate-type Seyfert galaxies (1.8/1.9) in between. Despite their low number, this is consistent with expectations and with similar studies in the literature (Risaliti et al. 1999).

It is also noteworthy that we do not find broad-line sources with high column density ($\log N_H/\text{cm}^2 \gtrsim 22.3$), such as Mrk 231, BAL QSOs, or the objects reported by Wilkes et al. (2002). The reason for this is probably that such objects are very rare. In optical spectra of all $\approx$570 AGNs in the BAT 70-month sample, Koss et al. (in prep.) find only nine optically unobscured AGNs with X-ray columns $\log N_H/\text{cm}^2 > 22.3$.

In conclusion, we find a consistent classification between optical and X-ray bands for our sample simply by choosing appropriate boundaries. If $\log N_H/\text{cm}^2 > 21.5$ (dashed lines in Fig. 2) is chosen for X-ray absorbed AGNs (as in e.g. Merloni et al. 2014), the corresponding boundary for "optically obscured" should be Seyfert $\geq$ 1.8. On the other hand, if Seyfert 1.8 and 1.9 are to be considered unobscured objects, then an absorbing column $\log N_H/\text{cm}^2 > 22.3$ (indicated by solid lines) should be used to classify objects as X-ray absorbed.

4. Optical obscuration and X-ray absorption

We can also directly look at the relation between the X-ray absorbing column and the optical extinction. Figure 3 summarizes our analysis, and shows a number of interesting features.

First, we find a general trend of increasing N_H with increasing A_V: type 1 sources are essentially unobscured both optically and in X-rays; intermediate Seyfert types (plotted in purple) show a variety of absorbing columns between unobscured and obscured sources; and optically obscured sources all have large absorbing columns ($\log N_H/\text{cm}^2 \gtrsim 22.3$). The only X-ray absorbed source with little optical obscuration (NGC 1052) is a LINER that shows broad lines in polarized light (Barth et al. 1999), i.e. it is not a true type 2 source (e.g. Panessa & Bassani 2002), but rather one with a peculiar absorbing geometry.

Within the large error of our A_V estimate, all sources lie above the Galactic ratio for which we assume a range of $(N_H/A_V)_{\text{galactic}} = (1.79\ldots2.69) \times 10^{21}\ \text{cm}^{-2}$ (Predehl & Schmitt 1995; Nowak et al. 2012). We find a wide spread in the observed N_H/A_V ratio with factors ranging from $\approx$1 (NGC 2992) to $\approx$200 $\times$ $(N_H/A_V)_{\text{galactic}}$ (NGC 1068).

The relation between optical extinction and X-ray absorption was first assessed in a systematic way by Goodrich et al. (1994) and Veilleux et al. (1997) and in many other more recent studies using various tracers for the optical extinction. Shi et al. (2006), for example, find a correlation (with large scatter) between the 9.7 μm silicate strength $\tau_{9.7}$ and the neutral gas column from X-ray observations in the sense that small columns correspond to silicate emission and large columns to silicate absorption. Lyu et al. (2014) study the relation between the Balmer decrement in the narrow line region and the Silicate strengths in a sample of $\sim$100 type 2 AGNs. There is almost no correlation between the two properties, which may be related to the fact that the Silicate absorption predominantly arises in the pc-scale torus while the narrow line region is much more extended.

Slightly higher N_H values than expected given the optical extinction or reddening have been known for a long time (Mushotzky 1982; Véron-Cetty & Véron 2000) and are also observed in the Galactic Centre (Porquet et al. 2008) (plotted in Fig. 3). In the following we discuss possible reasons for deviations from $(N_H/A_V)_{\text{galactic}}$.

4.1. Increased N_H/A_V due to modified dust?

Maiolino et al. (2001) used flux ratios between broad Balmer lines and computed the extinction towards the BLR assuming
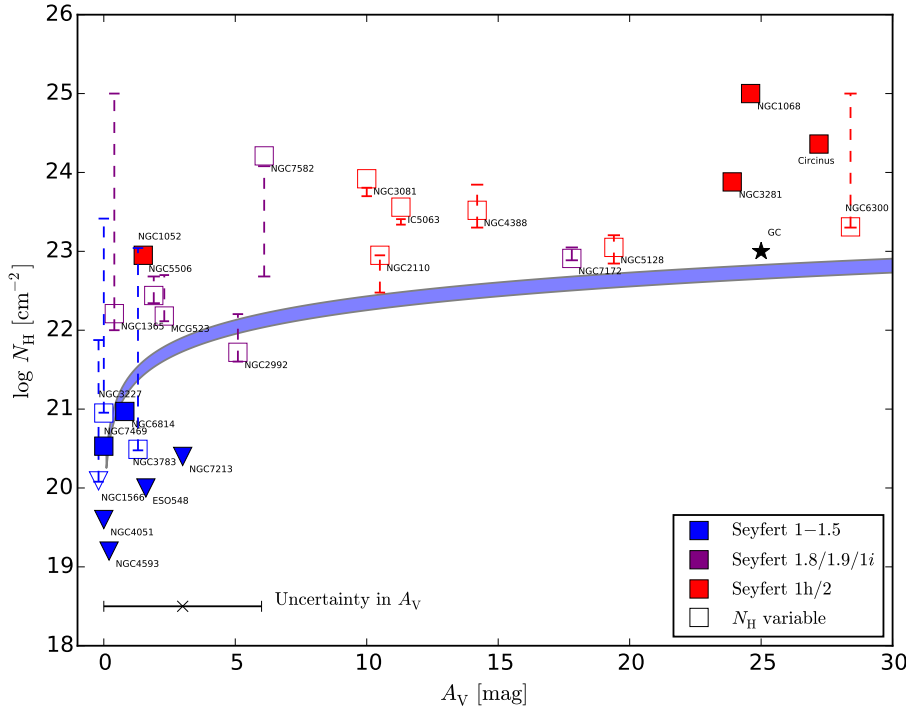
Fig. 3. N_H vs. A_V with Seyfert subtype labelled by colour. The blue band gives the Galactic standard ratio (see text for details). Open boxes indicate sources with variable N_H as listed in Table 1. The Galactic Centre is marked with an asterisk for comparison. Some sources with $A_V = 0$ have been slightly offset for clarity.

case B recombination is valid there. They find consistently higher values for N_H/A_V than expected from the Galactic diffuse interstellar medium and interpret these offsets as evidence for anomalous dust grains in the dense and extreme environments of galactic nuclei. The largest graphite grains can sustain higher temperatures than smaller silicate grains (e.g. Laor & Draine 1993). The sublimation radius is therefore a sublimation zone and observations have shown that the innermost dusty region is indeed at smaller radii than expected from models based on Galactic dust properties (Kishimoto et al. 2007; Barvainis 1987). However, this only affects the innermost zone of the dusty region and convincing evidence for altered dust properties in the bulk of the torus is not available.

4.2. Increased N_H/A_V due to dust-free neutral gas in the BLR?

An alternative explanation for the observed N_H/A_V ratios is that there is considerable absorption by neutral gas clouds inside the dust sublimation zone, as has been suggested by Granato et al. (1997). In fact, it is now observationally well established that the neutral absorbing column is variable in many, if not most, AGNs (e.g. Bianchi et al. 2012, and references therein). The prototypical sources NGC 1365 (Risaliti et al. 2009; Maiolino et al. 2010) and NGC 7582 (Bianchi et al. 2009) change between Compton-thin and reflection-dominated appearance within hours. Given the very short timescales, these variations must be caused by clouds in the BLR eclipsing the X-ray source. Further support for dust-free X-ray absorption comes from photoionization models by Netzer (2013), which show that the majority of the gas in BLR clouds is expected to be neutral.

In addition to these extreme "changing-look" sources, many more sources show changes in their absorbing columns over timescales of months and years. Some of these slower changes in the absorbing column may also be related to torus clumps passing our line of sight (Markowitz et al. 2014), but probably not all of them (e.g. Arévalo et al. 2014). We searched the literature

for all kinds of N_H variations for the sources in our sample. The range of reported N_H values is listed in Table 1 and is indicated in Fig. 3 by the dashed lines[4]. Compared to our fiducial value of N_H, i.e. the consistent analysis based on the spectral fitting in the 0.3–150 keV band by Ricci et al. (2015), the variability always changes N_H in the expected direction: for low fiducial N_H we find variability to values higher than the Galactic ratio and vice versa. We note that due to the variable nature of the gas column in most of the intermediate and obscured sources, the precise "fiducial" value of N_H is not very important for our conclusions.

It is actually striking to see that all six intermediate-type sources show variable gas columns (although for two the range is so small that this may also be due to calibration uncertainties). Since not all of the sources have been explored in the same detail, it is quite possible that for many other sources a large part of the gas column is more variable than indicated in the plot.

4.3. Reliability of our A_V estimate for the most obscured sources

Our A_V estimate relies on the assumption that the 2.3 μm continuum is dominated by emission from dust at the sublimation radius r_{sub}. For type 1 AGNs, this has indeed been shown by observations (e.g. Kishimoto et al. 2011). In the most obscured objects, however, the near-infrared emission from r_{sub} is probably obscured and we therefore see hot dust further away from the nuclear engine thanks to a direct sightline through the clumpy torus. In NGC 1068, for example, Speckle imaging and long-baseline infrared interferometry show that the hot dust is located on scales $\approx (3-10) \times r_{sub}$ (Weigelt et al. 2004; López-Gonzaga et al. 2014). This is also consistent with infrared searches for BLRs in obscured objects which have put large lower limits on

---

[4] For NGC 4388, Elvis et al. (2004) reported an uncovering event with an extremely low column of neutral gas ($\log N_H/cm^2 < 21.9$). We note, however, that their spectral fit also returns a very small photon index ($\Gamma < 1$), which is indicative of a more substantial column than given in that paper. We therefore do not show this value in Fig. 3.

A_V towards the BLR. For five of our type 2 objects, for example, Lutz et al. (2002) did not see a broad component of Brackett α (4.05 μm) implying $A_V > 50$. In heavily obscured sources, our A_V estimate is therefore only a lower limit of the actual A_V to the inner radius.

Even a twofold increase in the A_V of these sources, however, would not greatly reduce the offset these sources show from $(N_H/A_V)_{galactic}$. These sources must have substantial amounts of neutral gas columns within the dust-free BLR. This is consistent with X-ray observations of multiple thick absorbers along the line of sight (e.g. Arévalo et al. (2014) and Bauer et al. (2015) for the Circinus galaxy and NGC 1068, respectively).

4.4. Variability in Seyfert type or A_V?

Since the X-ray and infrared observations of our sample are not contemporaneous, how likely is it that deviations from $(N_H/A_V)_{galactic}$ are caused by variability in the optical obscuration of the AGNs? This question is difficult to tackle observationally because of the very long timescales involved. The crossing time for clouds that can obscure a substantial flux of the BLR for example, is at least a few years and likely much more (LaMassa et al. 2015). Furthermore, in the few, just recently discovered cases where such optical changing-look AGNs have been found by systematic searches in large archives, these changes are attributed to a change in the emission from the central engine rather than obscuring clouds passing by (Shappee et al. 2014; Ruan et al. 2015; Runnoe et al. 2016). Such major variations in the accretion flow seem to occur in roughly 1% of AGNs when comparing observations on a baseline of ten years (MacLeod et al. 2015). While it is not straightforward to attribute differences in the long-term optical obscuration of an AGN to eclipsing clouds, one can conclude that such changes are rare and therefore unlikely to be the cause of deviations from $(N_H/A_V)_{galactic}$ in our sample.

4.5. Could the obscuration be dominated by large-scale dust lanes?

Intermediate-type (1.8/1.9) Seyfert galaxies have been found to lie preferentially in edge-on galaxies and this has caused Maiolino & Rieke (1995) to suggest a distinct inner and outer torus, where the latter would be located in the plane of the galaxy and thus be responsible for the obscuration of these sources. This is in line with observations by Prieto et al. (2014) who have found that kpc-scale dust lanes can often be traced all the way to the central parsec and may be responsible for some of the obscuration seen in those galaxies. On the other hand, based on *Hubble* Space Telescope (HST) data of dust structures in a carefully controlled sample of active galaxies, Pogge & Martini (2002) did not find any evidence for differences in the large-scale structure of the various Seyfert subtypes. And on (sub-)parsec scales, mid-IR interferometry of about two dozen objects has shown that the dusty structures in type 1/2 Seyfert galaxies are indistinguishable in terms of size or mid-IR morphology (Burtscher et al. 2013).

The extinctions Prieto et al. (2014) found are only relatively small, in the range $A_V = 3$–6 mag. This is sufficient to obscure low luminosity nuclei, as the authors note, and for some of the less obscured sources in our sample this could be a relevant contribution. It may explain, for example, why the N_H/A_V ratio in NGC 2992 is very close to the Galactic ratio: owing to its rather

high inclination[5], its gas and dust column may be dominated by standard dust in the host galaxy rather than a possibly large dust-free gas column within the BLR.

Large-scale dust can therefore add some scatter to our relation at low extinctions, but will not significantly affect the general trend of increasing N_H with A_V over 30 orders of magnitude.

5. Conclusions

In this article we revisit the relation between optical obscuration and X-ray absorption in AGNs. We improve upon previous works by using a novel indicator for the optical obscuration – the temperature of the hot dust –, consistently estimated X-ray absorbing columns using 0.3–150 keV spectral energy distributions (Ricci et al. (2015).), by taking into account the variable nature of the neutral gas column N_H and by using a consistent classification of Seyfert subtypes. Our findings are summarized here:

– All BAT sources without hot dust detections are Compton-thick, but the inverse is not true: some of the most nearby Compton-thick objects show evidence for hot dust (the Circinus galaxy, NGC 1068 and NGC 7582).
– We have collected [OIII]λ5007/Hβ fluxes from the literature and determined the Seyfert subtype in a uniform manner using the widely used Winkler (1992) scheme. We find that a good correlation exists between Seyfert subtype and N_H and that a consistent classification between optical and X-ray appearance can be reached by choosing the thresholds appropriately. For example, if intermediate-type Seyfert galaxies (1.8/1.9) are considered optically unobscured, $\log N_H/cm^2 > 22.3$ must be required for sources to be X-ray absorbed.
– A relation exists between N_H and A_V, where the N_H/A_V ratio from the Galactic diffuse interstellar medium sets the lower limit. Within the errors, all AGNs lie above the relation as seen previously by e.g. Maiolino et al. (2001). By collecting data from the literature, we find that the X-ray absorbing columns in most of the intermediate and obscured AGNs in our sample are variable and their lower values are often nearly in agreement with the expected columns given the optical obscuration and the Galactic ratio. This suggests that the dust properties even in the extreme environment of AGNs can be similar to Galactic. In many sources, deviations from it may simply arise from variable neutral gas clouds within the BLR. This also shows that our dust colour method is a useful tool for deriving A_V in mildly obscured objects.
– In the most heavily obscured objects, however, we may underestimate the A_V towards the dust sublimation radius if the near-IR continuum originates from scales larger than r_{sub} – an issue that the second generation VLTI instrument GRAVITY (Eisenhauer et al. 2011) will resolve.
– We would encourage X-ray observers to look for significant gas column variability particularly in those sources that show large deviations from the Galactic N_H/A_V value, such as in NGC 3081, NGC 4388, or IC 5063.

---

5 Based on 2MASS (*K*-band) data, the galaxy's axis ratio $b/a = 0.43$, corresponding to an inclination of about 65 deg out of our line of sight.

References

Antonucci, R. R. J., & Miller, J. S. 1985, ApJ, 297, 621
Arévalo, P., Bauer, F. E., Puccetti, S., et al. 2014, ApJ, 791, 81
Astropy Collaboration, Robitaille, T. P., Tollerud, E. J., et al. 2013, A&A, 558, A33
Barth, A. J., Filippenko, A. V., & Moran, E. C. 1999, ApJ, 515, L61
Barvainis, R. 1987, ApJ, 320, 537
Bauer, F. E., Arévalo, P., Walton, D. J., et al. 2015, ApJ, 812, 116
Baumgartner, W. H., Tueller, J., Markwardt, C. B., et al. 2013, ApJS, 207, 19
Beckmann, V., Jean, P., Lubiński, P., Soldi, S., & Terrier, R. 2011, A&A, 531, A70
Bianchi, S., Piconcelli, E., Chiaberge, M., et al. 2009, ApJ, 695, 781
Bianchi, S., Maiolino, R., & Risaliti, G. 2012, Adv. Astron., 2012
Burtscher, L., Meisenheimer, K., Tristram, K. R. W., et al. 2013, A&A, 558, A149
Burtscher, L., Orban de Xivry, G., Davies, R. I., et al. 2015, A&A, 578, A47
Davies, R. I., Burtscher, L., Rosario, D., et al. 2015, ApJ, 806, 127
Dong, X., Wang, T., Wang, J., et al. 2008, MNRAS, 383, 581
Eisenhauer, F., Perrin, G., Brandner, W., et al. 2011, The Messenger, 143, 16
Elitzur, M. 2012, ApJ, 747, L33
Elvis, M., Risaliti, G., Nicastro, F., et al. 2004, ApJ, 615, L25
Fedorova, E. V., Beckmann, V., Neronov, A., & Soldi, S. 2011, MNRAS, 417, 1140
Goodrich, R. W., Veilleux, S., & Hill, G. J. 1994, ApJ, 422, 521
Goulding, A. D., Alexander, D. M., Bauer, F. E., et al. 2012, ApJ, 755, 5
Granato, G. L., Danese, L., & Franceschini, A. 1997, ApJ, 486, 147
Grupe, D., Wills, B. J., Leighly, K. M., & Meusinger, H. 2004, AJ, 127, 156
Guainazzi, M. 2002, MNRAS, 329, L13
Hicks, E. K. S., Davies, R. I., Malkan, M. A., et al. 2009, ApJ, 696, 448
Kawamuro, T., Ueda, Y., Tazaki, F., & Terashima, Y. 2013, ApJ, 770, 157
Kim, D.-C., Sanders, D. B., Veilleux, S., Mazzarella, J. M., & Soifer, B. T. 1995, ApJS, 98, 129
Kishimoto, M., Hönig, S. F., Beckert, T., & Weigelt, G. 2007, A&A, 476, 713
Kishimoto, M., Hönig, S. F., Antonucci, R., et al. 2011, A&A, 527, A121
LaMassa, S. M., Cales, S., Moran, E. C., et al. 2015, ApJ, 800, 144
Lamer, G., Uttley, P., & McHardy, I. M. 2003, MNRAS, 342, L41
La Mura, G., Popović, L. Č., Ciroi, S., Rafanelli, P., & Ilić, D. 2007, ApJ, 671, 104
Laor, A., & Draine, B. T. 1993, ApJ, 402, 441
Leighly, K. M., Halpern, J. P., Awaki, H., et al. 1999, ApJ, 522, 209
López-Gonzaga, N., Jaffe, W., Burtscher, L., Tristram, K. R. W., & Meisenheimer, K. 2014, A&A, 565, A71
Lumsden, S. L., Alexander, D. M., & Hough, J. H. 2004, MNRAS, 348, 1451
Lutz, D., Maiolino, R., Moorwood, A. F. M., et al. 2002, A&A, 396, 439
Lyu, J., Hao, L., & Li, A. 2014, ApJ, 792, L9
MacLeod, C. L., Ross, N. P., Lawrence, A., et al. 2015, MNRAS, submitted [arXiv:1509.08393]
Maiolino, R., & Rieke, G. H. 1995, ApJ, 454, 95
Maiolino, R., Marconi, A., Salvati, M., et al. 2001, A&A, 365, 28
Maiolino, R., Risaliti, G., Salvati, M., et al. 2010, A&A, 517, A47

Markowitz, A. G., Krumpe, M., & Nikutta, R. 2014, MNRAS, 439, 1403
Merloni, A., Bongiorno, A., Brusa, M., et al. 2014, MNRAS, 437, 3550
Moran, E. C., Barth, A. J., Kay, L. E., & Filippenko, A. V. 2000, ApJ, 540, L73
Müller-Sánchez, F., Prieto, M. A., Hicks, E. K. S., et al. 2011, ApJ, 739, 69
Mushotzky, R. F. 1982, ApJ, 256, 92
Nagar, N. M., Oliva, E., Marconi, A., & Maiolino, R. 2002, A&A, 391, L21
Netzer, H. 2013, The Physics and Evolution of Active Galactic Nuclei (Cambridge, UK: Cambridge University Press)
Netzer, H. 2015, ARA&A, 53, 365
Nowak, M. A., Neilsen, J., Markoff, S. B., et al. 2012, ApJ, 759, 95
Oliva, E., Marconi, A., Cimatti, A., & di Serego Alighieri, S. 1998, A&A, 329, L21
Osterbrock, D. E. 1977, ApJ, 215, 733
Osterbrock, D. E. 1981, ApJ, 249, 462
Osterbrock, D. E., & Ferland, G. J. 2006, Astrophysics of gaseous nebulae and active galactic nuclei, 2nd edn. (Sausalito, CA: University Science Books)
Panessa, F., & Bassani, L. 2002, A&A, 394, 435
Phillips, M. M., Charles, P. A., & Baldwin, J. A. 1983, ApJ, 266, 485
Pogge, R. W., & Martini, P. 2002, ApJ, 569, 624
Porquet, D., Grosso, N., Predehl, P., et al. 2008, A&A, 488, 549
Predehl, P., & Schmitt, J. H. M. M. 1995, A&A, 293, 889
Prieto, M. A., Mezcua, M., Fernández-Ontiveros, J. A., & Schartmann, M. 2014, MNRAS, 442, 2145
Ramos Almeida, C., Levenson, N. A., Alonso-Herrero, A., et al. 2011, ApJ, 731, 92
Ramos Almeida, C., Martinez Gonzalez, M. J., Asensio Ramos, A., et al. 2015, MNRAS, submitted
Rees, M. J. 1966, Nature, 211, 468
Reunanen, J., Kotilainen, J. K., & Prieto, M. A. 2003, MNRAS, 343, 192
Ricci, C., Ueda, Y., Koss, M. J., et al. 2015, ApJ, 815, L13
Risaliti, G., Maiolino, R., & Salvati, M. 1999, ApJ, 522, 157
Risaliti, G., Elvis, M., & Nicastro, F. 2002, ApJ, 571, 234
Risaliti, G., Salvati, M., Elvis, M., et al. 2009, MNRAS, 393, L1
Rivers, E., Markowitz, A., Rothschild, R., et al. 2014, ApJ, 786, 126
Ruan, J. J., Anderson, S. F., Cales, S. L., et al. 2015, ApJ, submitted [arXiv:1509.03634]
Runnoe, J. C., Cales, S., Ruan, J. J., et al. 2016, MNRAS, 455, 1691
Schartmann, M., Meisenheimer, K., Camenzind, M., et al. 2008, A&A, 482, 67
Schmitt, H. R., Donley, J. L., Antonucci, R. R. J., Hutchings, J. B., & Kinney, A. L. 2003, ApJS, 148, 327
Shappee, B. J., Prieto, J. L., Grupe, D., et al. 2014, ApJ, 788, 48
Shi, Y., Rieke, G. H., Hines, D. C., et al. 2006, ApJ, 653, 127
Shi, Y., Rieke, G. H., Smith, P., et al. 2010, ApJ, 714, 115
Shields, J. C., & Filippenko, A. V. 1996, A&A, 311, 393
Smajić, S., Fischer, S., Zuther, J., & Eckart, A. 2012, A&A, 544, A105
Smith, J. E., Robinson, A., Alexander, D. M., et al. 2004, MNRAS, 350, 140
Storchi-Bergmann, T., Bica, E., & Pastoriza, M. G. 1990, MNRAS, 245, 749
Tadhunter, C. N., Morganti, R., di Serego-Alighieri, S., Fosbury, R. A. E., & Danziger, I. J. 1993, MNRAS, 263, 999
Tran, H. D. 2001, ApJ, 554, L19
Veilleux, S., Goodrich, R. W., & Hill, G. J. 1997, ApJ, 477, 631
Véron-Cetty, M., & Véron, P. 2010, A&A, 518, A10
Véron-Cetty, M. P., & Véron, P. 2000, A&ARv, 10, 81
Walton, D. J., Risaliti, G., Harrison, F. A., et al. 2014, ApJ, 788, 76
Weigelt, G., Wittkowski, M., Balega, Y. Y., et al. 2004, A&A, 425, 77
Whittle, M. 1992, ApJS, 79, 49
Wilkes, B. J., Schmidt, G. D., Cutri, R. M., et al. 2002, ApJ, 564, L65
Winkler, H. 1992, MNRAS, 257, 677